Surface Tension Prediction of n-Alkanes by a Modified Peng-Robinson Equation of State Using the Density Functional Theory

N. Farzi[a],* and Z. Yazdanshenas[b]

[a]Department of Chemistry, University of Isfahan, Isfahan, Iran
[b]Department of Chemistry, Payame Noor University, P.O. Box: 19395-3697, Tehran, Iran
(Received 28 December 2016, Accepted 29 April 2017)

   Through this study, the ability of a modified Peng-Robinson (MPR) equation of state in predicting the surface tension of n-alkanes based on the density functional theory approach was investigated and compared with other studies. The interfacial layer thickness and the density profile were calculated simultaneously at different temperatures from triple point to near critical point using the modified Peng-Robinson equation of state. It was shown that the calculated thickness of interfacial layer increases with decrease in the chain length of n-alkane molecules and raising of temperature. The surface tension of n-alkanes was calculated using the calculated values of thin layers' densities. It was shown that the calculated surface tension of n-alkanes decreases with temperature in accordance with the experiment. The average relative error in prediction of the surface tension by the MPR equation of state was in the range of 2.5-6% while it was 4.6-25.2% by the Peng-Robinson equation of state. The validity of the MPR equation of state in the surface tension prediction of n-alkanes containing C_1-C_{10} has been proved by comparing the results of this work with other studies.

Keywords: Surface tension, Density functional theory, n-Alkanes, Density profile

INTRODUCTION

   A macroscopic thermodynamic property related to the microscopic structure of molecules in the vapor-liquid interface is the surface tension which is the result of an imbalance of intermolecular forces. The difference between the intermolecular interactions in the bulk and at the surface is related to the order and the structure of molecules. The surface tension has an important effect on mass and energy transfer because of the dependency of surface energy on the intermolecular forces, density, and molecular size.

   Surface tension is a thermophysical property that has many industrial applications such as liquid-liquid, and condensation. For this reason, an accurate estimation of the surface tension is needed [1].

   The surface tension of fluids has been frequently studied experimentally and theoretically. Several empirical and semi-empirical correlations have been presented for predicting surface tension [2-5]. Along with the development of various empirical correlations for surface tension of pure substances and mixtures, the modeling of surface tension has progressed.

   Parachor method [6,7], alongside the law of corresponding states [8,9], perturbation theory [10,11], Gradient theory [12,13], and density functional theory (DFT) [14,15] are the theoretical models which have been frequently used in predicting surface tension. Among them, DFT is widely applied to describe the surface phenomena. Simple classical fluids, dipolar fluids, liquid metals, associating and polyatomic molecules, and heavy water are examples whose interfacial properties are investigated by DFT method [16,17] .

   DFT method was also used to calculate the surface tension with a simple renormalization formalism in critical point [18]. DFT was combined with equations of state

---

*Corresponding author. E-mail: nfarzi@sci.ui.ac.ir

(EoSs) for predicting the interfacial properties of fluids [19-21]. The vapor-liquid interfacial tension of non-associating and associating fluids have been predicted using SAFT-DFT approach by Gloor, *et al.* [17,22,23]. Kahl, *et al.* [24] predicted the surface properties and phase equilibria of non-associated fluids using the modified PT-LJ-SAFT DFT. Gross, used the DFT for vapor-liquid interfaces using the PCP-SAFT EoS [25]. Maghari *et al.* employed DFT with the modified SAFT-BACK EoS to investigate the liquid-vapor interfaces of n-alkanes [19]. Moreover, Llovell *et al.* applied the SAFT-VR DFT in the prediction of the interfacial properties of fluids mixtures [26,27]. Last but not least, Von Müller, *et al.* used the PCP-SAFT-DFT formalism for surface tension calculations [21].

In this work, the ability of a modified Peng-Robinson (MPR) EoS [28] in predicting surface tensions of n-alkanes was investigated using the DFT approach and compared with the Peng-Robinson (PR) EoS [29]. In fact, the extent to which the calculated surface tension by MPR EoS is reliable was investigated. The parameter b in the PR EoS has been modified as the function of reduced temperature, $T_r = T/T_C$, and acentric factor, ω, by Feyzi *et al.* in the MPR EoS. The modified parameter b can be used in other cubic EoSs. The PR EoS was frequently used in predicting the surface tension of some pure substances and their mixtures by different methods such as the law corresponding states [9] and gradient theory [12]. Li and Firoozabadi [20] also developed a DFT-based technique through combination of the PR EoS, the weighted density approximation (WDA) and quadratic density expansion (QDE). The theory led to the PR EoS in the bulk limit. This method was used for predicting the surface tension of some pure substances including n-alkanes. A good agreement between the calculated surface tension and the experimental values indicates that the use of QDE could compensate the weakness of the PR EoS in predicting density.

In the present study, the MPR EoS has been used for the prediction of the surface tension of n-alkanes with the DFT approach. The surface region was divided into many thin layers and the density of each layer was predicted by the MPR EoS. In the DFT approach, the density gradient, the surface thickness and the heterogeneity are taken into account. Therefore, in addition to the surface tension, the density profile and the thickness of interfacial layer were calculated for n-alkanes using the PR and MPR EoSs.

EQUATIONS OF STATE

The equations of state that can predict the phase behavior and the volumetric properties of different fluids are very important in chemical engineering. In this work, the PR and MPR EoSs were used in predicting the surface tension of n-alkanes. The PR EoS is given by [29]:

$$P = \frac{RT}{(V-b)} - \frac{a}{(V^2 + 2bV - b^2)} \tag{1}$$

where R, T and V are the universal constants of gases, temperature and the molar volume, respectively. The temperature-dependent parameters of the PR EoS, a and b, are calculated using the critical temperature and pressure, T_c and P_c, as:

$$a = \alpha \left(0.45724 \frac{R^2 T_c^2}{P_C} \right) \tag{2}$$

$$b = \beta \left(0.07780 \frac{RT_C}{P_C} \right) \tag{3}$$

where the parameter b has a constant value for each fluid and β is equal to 1. The parameter α is a function of the reduced temperature, $T_r = T/T_C$, and acentric factor, ω, is given by:

$$\alpha^{1/2} = 1 + \left(0.37464 + 1.54226\omega - 0.26992\omega^2 \right)\left(1 - T_r^{1/2} \right) \tag{4}$$

The PR EoS was frequently used in research and industrial design due to its simplicity and acceptable precision. Despite significant developments in EoSs, the PR EoS and its modified versions are used as efficient tools in calculation the properties of fluids.

Unlike the PR EoS, the parameters α and β in the MPR EoS [28] are functions of T_r and ω as well. The modified parameter α, is given for all T_r as:

$$\alpha^{1/2} = 1 + [-0.03049 + \left(0.61991 - 0.39384\omega + 0.69849\omega^2 \right)\left(1 - T_r \right) + \\ \left(-0.44656 + 1.95484\omega - 1.80666\omega^2 \right)\left(1 - T_r \right)^2][1 - \exp(-100|T_r - 1|)] \tag{5}$$

while the parameter β in $T_r \leq 0.97$ or $T_r \geq 1.03$ is given by:

$$\beta^{1/2} = 0.95514 + \left(0.61013 - 1.418143\omega + 0.94321\omega^2\right)\left(1 - T_r\right) + \left(-0.81945 + 2.11084\omega - 1.75858\omega^2\right)\left(1 - T_r\right)^2 \tag{6}$$

and near the critical point ($0.97 \leq T_r \leq 1.03$), β is given by:

$$\beta^{1/2} = \left(0.999 + 0.00872\omega - 0.02733\omega^2\right)^{1/2}\left[-0.044861 + \left(0.61013 - 1.41814\omega + 0.94321\omega^2\right)\left(1 - T_r\right) + \left(-0.81945 + 2.11084\omega - 1.75858\omega^2\right)\left(1 - T_r\right)^2\right]\left[1 - \exp(-100\,|T_r - 1|)\right] \tag{7}$$

It can be shown that the accuracy of the predicted vapor pressure and density values of fluids by the MPR EoS [28] is more than those by the PR EoS. The predicted values of vapor pressure and liquid-vapor volumes of methane and ethane by the PR and MPR EoSs were compared with their experimental values [30,31] in Table 1.

THEORY

DFT and Surface Tension

Modern DFT, for quantum as well as classical systems, is based on the theorems of Hohenberg and Kohn [33]. The Hohenberg-Kohn theorems apply specifically to the ground state energy, and, therefore, only at zero absolute temperature. It is needed to extend these theorems to non-zero temperature for statistical mechanic applications. Mermin [34] showed that for a system at fixed temperature, T, the chemical potential, μ, and the external single-particle potential, $\upsilon(r)$, there is a functional $F[\rho(r)]$, independent of $\upsilon(r)$ and μ, so that the functional:

$$\Omega\left[\rho(r)\right] = F\left[\rho(r)\right] + \int dr\left[\upsilon(r) - \mu\right] \tag{8}$$

is a minimum for the correct equilibrium density $\rho(r)$ subject to the external potential. The value of Ω at this minimum is the grand potential. For systems restricted to constant density, minimization of the functional F gives the equilibrium Helmholtz potential.

The grand potential function in the absence of an external potential is given by:

$$\Omega\left[\rho(r)\right] = F\left[\rho(r)\right] + \int \mu\rho(r)dr \tag{9}$$

or

$$\Omega\left[\rho(r)\right] = \int\left[F\left[\rho(r)\right] - \rho(r)\mu\right]dr \tag{10}$$

Here, $F[\rho(r)]$ is the intrinsic Helmholtz free energy functional containing the ideal gas term and all contributions from the intermolecular interactions.

DFT is useful not only for inhomogeneous systems that are subject to an external field but also for uniform systems such as conventional bulk vapor and liquid phases, and for anisotropic fluids such as liquid crystals.

The grand potential function, $\Omega[\rho(r)]$, is the appropriate function for an inhomogeneous fluid at constant temperature and chemical potential. The minimum value of $\Omega[\rho(r)]$ is the grand potential of the system. Among all possible density profiles $\rho(r)$, the equilibrium density profile $\rho(r)$ is the one that minimizes the grand potential with:

$$\frac{\partial\Omega\left[\rho(r)\right]}{\partial\rho(r)} = 0 \tag{11}$$

and the chemical potential is obtained by

$$\mu = \frac{\partial F\left(\rho_0(r)\right)}{\partial\rho_0(r)} \tag{12}$$

The differential of grand potential functional, $d\Omega$ at constant temperature and zero external potential can be given by:

$$d\Omega = \gamma dA - pdV \tag{13}$$

where γ and P are the surface tension and the vapor pressure, respectively.

If the surface region is divided into many thin layers with dz thickness and dA surface, the surface tension of ith layer can be expressed by:

Table 1. Comparison of the Calculated Values for the Vapor Pressure, P, Liquid and Vapor Volumes, V_l and V_v, by the PR and MPR EoSs with their Experimental Values [31,32]. The Experimental and the Calculated Values were Rounded to Two Decimal Places

Alkane	T (K)	Property	Experiment	Calculated			
				PR EoS	ARD (%)[a]	MPR EoS	ARD (%)
CH$_4$	100	P (kPa)	34.00	35.22	3.59	33.95	0.15
		V_l (cm^3 mol^{-1})	36.43	32.13	11.82	36.05	1.06
		V_v (cm^3 mol^{-1})	24079.04	23265.04	3.38	24150.77	0.30
	140	P (kPa)	637.50	652.40	2.34	652.20	2.30
		V_l (cm^3 mol^{-1})	42.24	38.26	9.42	43.41	2.76
		V_v (cm^3 mol^{-1})	1599.41	1551.80	2.98	1529.61	4.36
C$_2$H$_6$	163.15	P (kPa)	28.22	27.70	1.84	27.10	3.97
		V_l (cm^3 mol^{-1})	55.62	48.16	13.41	52.42	5.77
		V_v (cm^3 mol^{-1})	52262.55	48424.30	7.34	49452.00	5.38
	173.15	P (kPa)	54.21	53.43	1.44	53.26	1.75
		V_l (cm^3 mol^{-1})	53.81	49.15	8.66	53.86	0.08
		V_v (cm^3 mol^{-1})	28013.16	26444.10	5.60	26489.20	5.44

[a]The percentage of absolute relative deviation: $ARD\% = \dfrac{\left|Z^{exp} - Z^{cal}\right|}{Z^{exp}} \times 100$.

$$\gamma_i = \frac{d\Omega[\rho_0(r)] + pdv}{dA} \tag{14}$$

or

$$\gamma_i = \frac{d\Omega[\rho_0(r)] + pdv}{dV} dz \tag{15}$$

Therefore, the total surface tension can be calculated by sum over total layers as:

$$\gamma = \int_{-\infty}^{\infty}\left[\frac{d\Omega[\rho_0(z)]}{dV} + P\right]dz \approx \sum_{i=1}^{n}\left[\frac{\Delta\Omega[\rho_0(z)]}{\Delta V} + P\right]\Delta z_i \tag{16}$$

Using the Eq. (10), we have:

$$\frac{\Delta\Omega[\rho_0(z)]}{dV} = f[\rho_0(z)] - \rho_0(z)\mu \tag{17}$$

where $f[\rho_0(r)] = F[\rho_0(r)]/V$ and the chemical potential is obtained from the classical thermodynamic relation as:

$$\mu = F + NkTZ \tag{18}$$

where Z is the compressibility factor and N is the number of molecules. Replacement of $f[\rho_0(z)]$ and μ into Eq. (17) leads to a surface tension as follows:

$$\gamma = \int_{-\infty}^{\infty} \big[P - P[\rho_0(z)] \big] dz \approx \sum_{i=1}^{n} \big[P - P[\rho_0(z)] \big] \Delta z_i \tag{19}$$

where the EoS can be used for calculating $P[\rho_0(z)]$ while knowing the density in each layer.

Density Profile and Interfacial Thickness

The fluid in the surface is considered as an inhomogeneous fluid. When the surface region is divided into n thin layers with dz thickness, a density gradient exists in the vertical direction of the surface, $\rho(z)$. However, it is assumed that there is no density gradient in horizontal direction of the surface. The functional form of density with the distance from the hypothetical dividing surface in z_0 was given by Rowlinson & Widom [35] as:

$$\rho(z) = \frac{1}{2}(\rho_l + \rho_v) - \frac{1}{2}(\rho_l - \rho_v)\tanh\big[2(z - z_0)/t\big] \tag{20}$$

where ρ_l and ρ_v are the liquid and vapor densities, respectively, and t stands for the surface thickness. The density in z_0 is given by,

$$\rho(z_0) = \frac{1}{2}(\rho_l + \rho_v) \tag{21}$$

where ρ_l and ρ_v can be obtained from the following equilibrium conditions:

$$\begin{aligned} (F + PV)_l &= (F + PV)_v \\ (Z\rho kT)_l &= (Z\rho kT)_v \end{aligned} \tag{22}$$

where F and Z are Helmholtz free energy and the compressibility factor, respectively. The density in each layer is treated as the average density:

$$\rho(z_i) = \frac{\int_{z_i}^{z_{i+1}} \rho(z)dz}{z_{i+1} - z_i} \qquad (i = 1, \dots, n) \tag{23}$$

where the subscript i is the number of each layer and n is the total number of the layers.

RESULTS AND DISCUSSION

Calculation of the Interfacial Density

The equilibrium pressure and the densities of the liquid and vapor phases, ρ_l and ρ_v, at different temperatures were calculated for n-alkanes including C_1-C_{10} using the equilibrium conditions, Eq. (22), and the PR and MPR EoSs. The thickness of interfacial layer was divided into 400 equal thin layers. Then, the density of the dividing layer was calculated by Eq. (21) for the n-alkanes that were examined at different temperatures. The density of each thin layer and the thickness of interfacial layer were calculated by solving the simultaneous equations for the density of the interfacial thin layers using Eqs. (20) and (23) for n-alkanes including C_1-C_{10} at different temperatures. All calculations were performed from the triple point up to around critical point, as a result of lacking experimental surface tension data at low temperatures and near critical region. Figure 1 typically shows the density profile of the interfacial layer of n-decane in the temperature range from 243.5-550 K.

It is clear from Fig. 1 that the interfacial layer thickness, t, increases with temperature, while the difference between the liquid and vapor densities decreases which is congruent with the literature [36-38]. The variation of the interfacial layer thickness with temperature has been shown in Fig. 2 for n-alkanes including C_1-C_{10}. As demonstrated, the thickness of the interfacial layer increases with temperature for all n-alkanes and the slope of the interfacial layer thickness plots versus temperature decreases with increasing the chain length of n-alkanes molecules. In other words, the results show that the interfacial layer thickness increases with decreasing of chain length in a constant temperature. This can be attributed to the weak interaction of the short chain alkane molecules with respect to the long chain alkanes.

Calculation of the Surface Tension of n-Alkanes (C_1-C_{10})

As mentioned before, the surface tension can be calculated by DFT approach using EoS according to Eq. (19). In this work, the surface tensions of n-alkanes (C_1-C_{10})
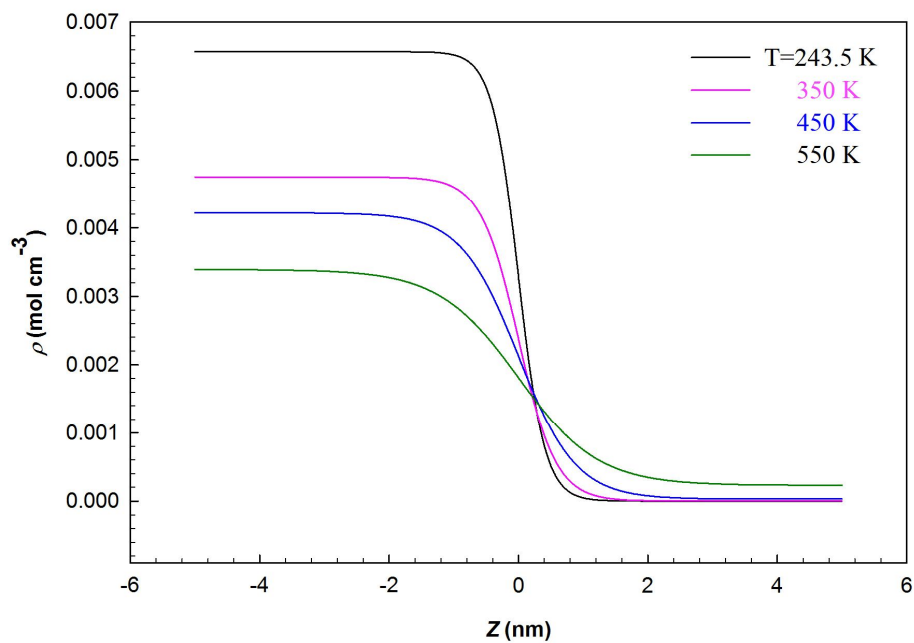
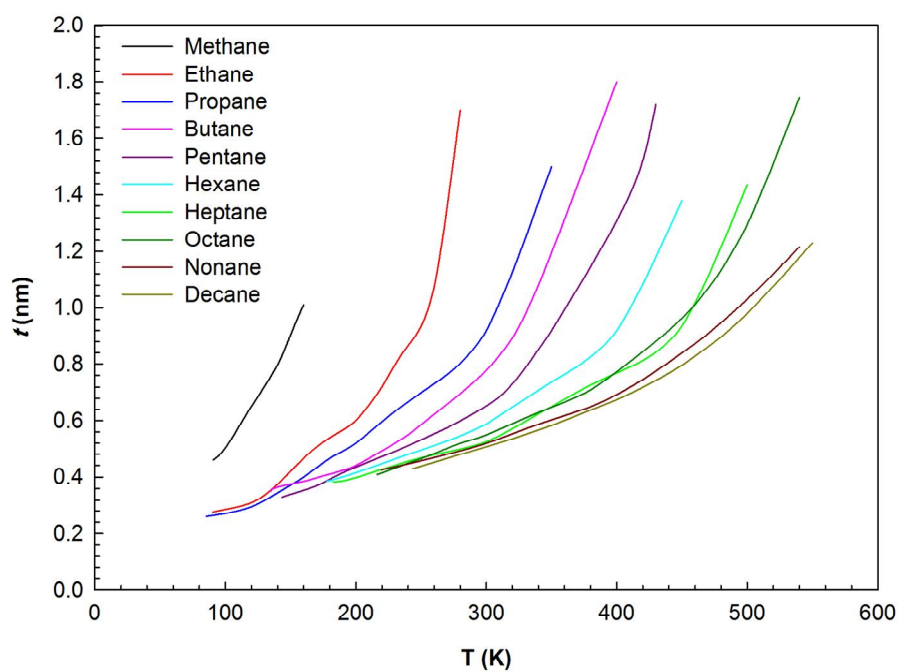**Fig. 1.** The obtained density profiles for n-decane at different temperatures.

Fig. 2. Variation of the interfacial layer thickness, t, with temperature for n-alkanes C_1-C_{10}.

Table 2. Comparison of the Calculated Surface Tension, γ_{cal}, of n-Alkanes (C_1-C_{10}) by PR and MPR EoSs with the experiment [39], γ_{exp}, at Different temperatures Along with their Percentage of Absolute Relative Deviation (ARD%)

Alkane	T (K)	γ_{exp} (mN m^{-1})	γ_{cal} (mN m^{-1})			
			PR EoS	ARD (%)	MPR EoS	ARD (%)
	90.69	18.76	21.10	12.50	19.22	2.45
	100	16.25	18.93	16.49	16.48	1.41
CH$_4$	120	11.31	14.85	31.30	12.07	6.72
	140	7.05	9.40	33.33	7.47	5.96
	150	5.19	6.90	32.95	5.57	7.32
	160	3.52	4.40	25.00	3.73	5.96
	90.35	31.67	29.17	7.89	32.94	4.01
	100	30.04	27.34	9.00	29.69	1.17
	120	26.68	25.63	3.93	25.91	2.89
	140	23.33	22.88	1.93	21.80	6.56
	160	20.05	21.86	9.03	19.87	0.89
C$_2$H$_6$	180	16.77	18.89	12.64	16.59	1.07
	200	13.59	14.88	9.49	12.79	5.88
	220	10.5	11.79	12.28	10.70	3.81
	240	7.56	8.37	10.71	7.32	3.17
	260	4.80	5.06	5.42	4.73	1.46
	280	2.32	2.54	9.48	2.89	24.57
	85.48	37.71	32.06	14.98	38.5	2.10
	100	35.43	29.53	16.66	33.88	4.36
	120	32.32	27.21	15.79	29.5	8.72
	140	29.24	26.64	8.88	27.46	6.07
	160	26.20	25.57	2.40	25.23	3.66
C$_3$H$_8$	180	23.20	24.24	4.45	23.07	0.57
	200	20.26	21.68	7.00	20.042	1.08
	250	13.20	14.64	10.90	13.04	1.23
	300	6.76	6.67	1.28	6.20	8.26
	350	1.39	0.91	34.31	1.34	3.70

Table 2. Continued

	134.89	33.49	31.83	4.96	34.62	3.37
	140	32.75	31.94	2.47	34.39	5.01
	160	29.88	28.85	3.44	29.96	0.27
	180	27.07	26.9	3.58	26.26	3.06
n-C_4H_{10}	200	24.32	23.54	3.20	23.03	5.30
	240	19.01	19.9	4.70	18.68	1.72
	300	11.60	13.03	12.30	12.00	3.43
	340	7.14	8.51	19.19	8.12	13.72
	400	1.53	1.28	16.34	1.82	18.95
	143.47	33.09	29.76	10.06	32.60	1.55
	150	32.33	29.34	9.25	31.82	1.58
	170	30.01	27.79	7.39	29.32	2.29
	190	27.69	26.96	2.64	27.74	0.18
	230	23.09	23.24	0.65	22.95	0.60
n-C_5H_{12}	270	18.57	18.96	2.1	18.21	1.93
	310	14.18	14.56	2.67	13.83	2.47
	350	9.97	11.13	11.63	10.69	7.22
	410	4.23	4.03	4.66	4.36	3.07
	430	2.54	2.39	5.90	2.94	15.75
	177.83	31.96	28.95	9.42	30.94	3.19
	200	29.26	26.91	8.03	28.13	3.86
	250	23.35	22.35	4.28	22.47	3.77
n-C_6H_{14}	300	17.74	17.31	2.42	16.99	4.23
	350	12.49	12.66	1.36	12.39	0.80
	400	7.70	7.52	2.36	7.59	1.45
	450	3.50	3.34	4.62	3.81	8.79
	182.55	33.10	28.89	12.72	31.28	5.50
	200	31.01	27.85	10.51	29.74	4.10
	250	25.25	23.22	8.04	24.00	4.95
	300	19.83	18.55	6.45	18.76	5.39
n-C_7H_{16}	350	14.75	13.70	7.11	13.75	6.78
	400	10.45	9.56	8.52	9.72	6.98
	450	5.77	4.94	14.38	5.31	7.97
	500	2.10	1.65	21.43	2.21	5.24

Table 2. Continued

	216.37	29.32	25.82	11.93	27.75	5.35
	220	28.94	25.57	11.64	27.43	5.22
	240	26.89	24.44	9.11	25.94	3.53
	260	24.88	23.14	6.99	24.32	2.25
	280	22.91	21.81	4.80	22.74	0.74
n-C_8H_{18}	300	20.98	20.00	4.67	20.71	1.28
	340	17.28	16.64	3.70	17.08	1.16
	380	13.63	13.29	4.99	12.95	2.49
	420	10.20	10.07	4.95	9.70	1.27
	460	6.97	6.82	8.89	6.35	2.15
	500	3.98	3.92	15.83	3.35	1.51
	540	1.37	1.32	41.39	0.83	3.65
	219.7	30.14	26.90	10.75	29.40	2.45
	260	26.12	23.37	10.52	25.10	3.90
	300	22.24	20.08	6.34	21.258	4.31
	340	18.51	17.00	8.16	17.85	3.56
n-C_9H_{20}	380	14.92	13.45	9.85	14.10	5.49
	420	11.50	10.36	9.91	10.94	4.87
	460	8.29	7.32	11.7	7.89	4.82
	500	5.31	4.36	17.89	4.92	7.34
	540	2.66	1.75	34.21	2.43	8.64
	243.5	28.50	24.20	17.77	26.64	6.98
	300	23.19	20.46	13.34	22.11	4.88
	350	18.69	16.75	11.58	17.93	4.24
n-$C_{10}H_{22}$	400	14.40	12.96	11.11	13.85	3.97
	450	10.37	9.23	12.35	9.97	4.01
	500	6.63	5.73	15.70	6.40	3.59
	550	3.30	2.45	34.69	3.03	8.91

have been obtained using the calculated densities of the interfacial thin layers and both the PR and MPR EoSs. The results have been demarcated in Table 2. According to the results, the predicted surface tensions of all n-alkanes, using the PR and MPR EoSs, decrease with temperature. Comparison of the experimental values [39] and the predicted surface tension values using the PR and MPR EoSs shows that the MPR EoS better predicts the surface tensions of n-alkanes with a good accuracy in the range of experimental errors. The average of relative errors in calculation of the surface tension by the PR and MPR EoSs is given in Table 3. As seen, the maximum average absolute

Table 3. The Percentage of Average Absolute Relative Deviation, AARD%, in Calculation of the Surface Tension by PR-DFT and MPR-DFT in the Given Temperature Range, ΔT

Alkane	ΔT (K)	Data point of γ	AARD (%)[a]	
			PR EoS	MPR EoS
CH_4	90.69-160	6	25.26	4.97
C_2H_6	90.35-280	11	8.34	5.04
C_3H_8	85.48-350	10	15.52	3.98
n-C_4H_{10}	134.89-400	9	7.80	6.09
n-C_5H_{12}	143.47-430	10	5.69	3.66
n-C_6H_{14}	177.83-450	7	4.64	3.73
n-C_7H_{16}	182.55-500	8	11.15	5.86
n-C_8H_{18}	216.37-540	12	10.57	2.55
n-C_9H_{20}	219.70-540	9	13.26	5.05
n-$C_{10}H_{22}$	243.50-555	7	16.65	5.23

[a]The percentage of average absolute relative deviation in the surface tension calculation:

$$AARD\% = \frac{1}{N}\sum_{i=1}^{N}\frac{\left|\gamma_{i,cal} - \gamma_{i,exp}\right|}{\gamma_{i,exp}}\times 100$$

relative deviation in calculation of surface tension using the MPR EoS is nearly 6% while it is 25% using the PR EoS. Due to the fact that the accuracy of the calculated surface tension strongly depends on the accuracy of the determined interfacial thin layers densities, a good agreement between the calculated surface tension and the experimental values signifies the accuracy of the obtained density profile for n-alkanes.

In addition to the DFT method, the surface tensions of n-alkanes were studied by other theoretical methods. However, it seems that the DFT method gives more appropriate results. Figures 3a and 3b compare the percentage of absolute relative deviation values in prediction of the surface tension of C_6H_{14} and $C_{10}H_{22}$ by the present work (MPR-DFT and PR-DFT) with the molecular dynamics simulation results calculated using different models [40-42]. As seen, MPR-DFT could better predict the surface tension of C_6H_{14} and $C_{10}H_{22}$.

The present research has been also compared in Fig. 4 with another PR-DFT study [20] which uses some approximation in the excess Helmholtz energy function. It is clear that the MPR-DFT results calculated in this work are in agreement with the experiment and other PR-DFT studies [20] that use some approximation. This implies that the acceptable results can be obtained for surface tension of n-alkanes without any further assumption using the MPR-DFT method.

The MPR and PR EoSs can be also compared with the other EoSs in prediction of the surface tension of n-alkanes. Figure 5 compares the calculated surface tensions of n-alkanes by the MPR-DFT and PR-DFT with the SAFT-BACK-DFT results [19]. A seen, the PR-DFT model cannot fairly predict the surface tension of alkanes compared to MPR-DFT and SAFT-BACK-DFT models. Moreover, the predicted surface tension by MPR-DFT is comparable with
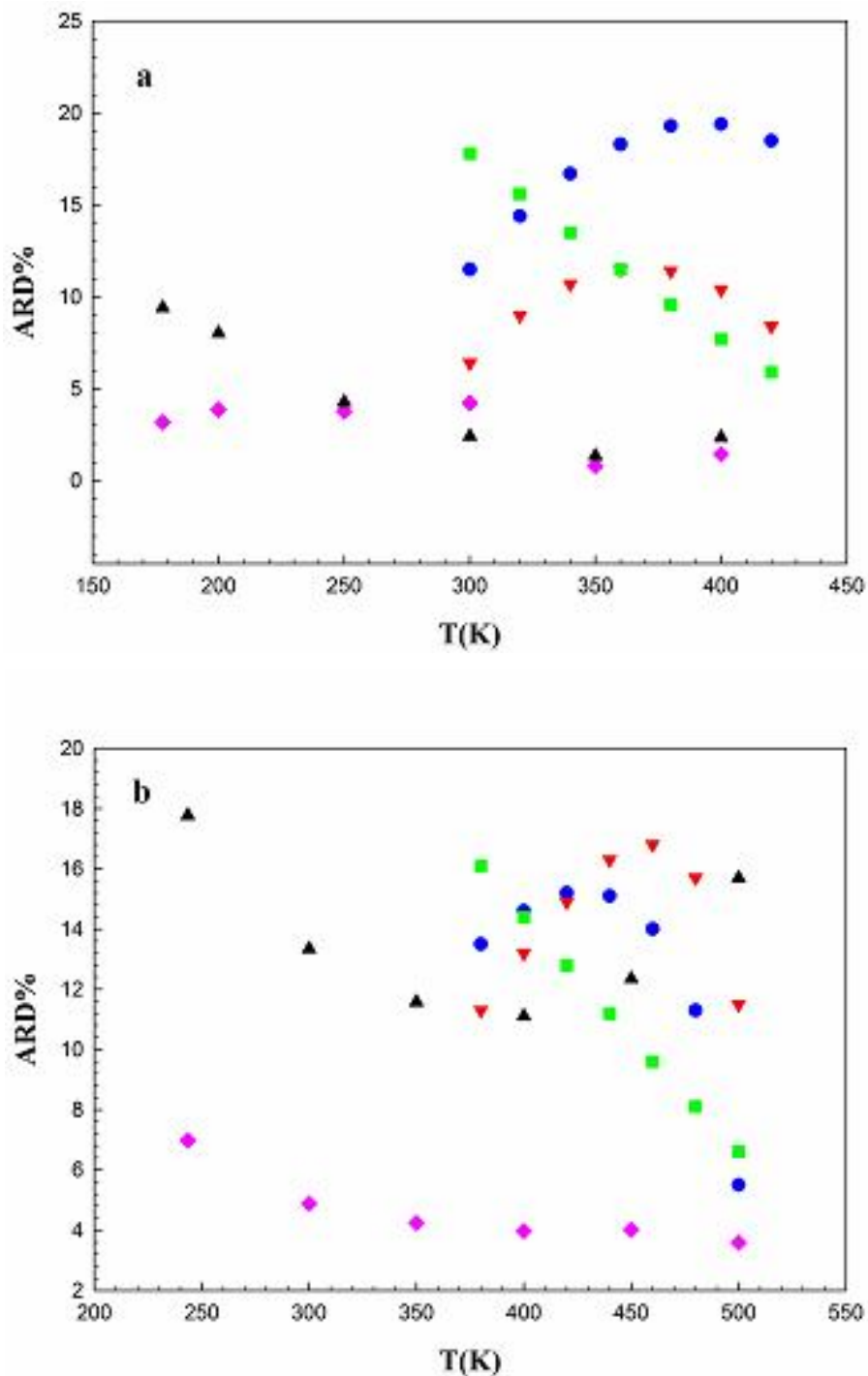
Fig. 3. Comparison of the absolute relative deviation percentage (ARD%) in the surface tension prediction by this work; PR-DFT (▲) and MPR-DFT (♦); the molecular dynamics simulation results calculated by different models [40-42]; TraPPE (▼), NERD (●) and UA (■); for a) C_6H_{14} and b) $C_{10}H_{22}$.
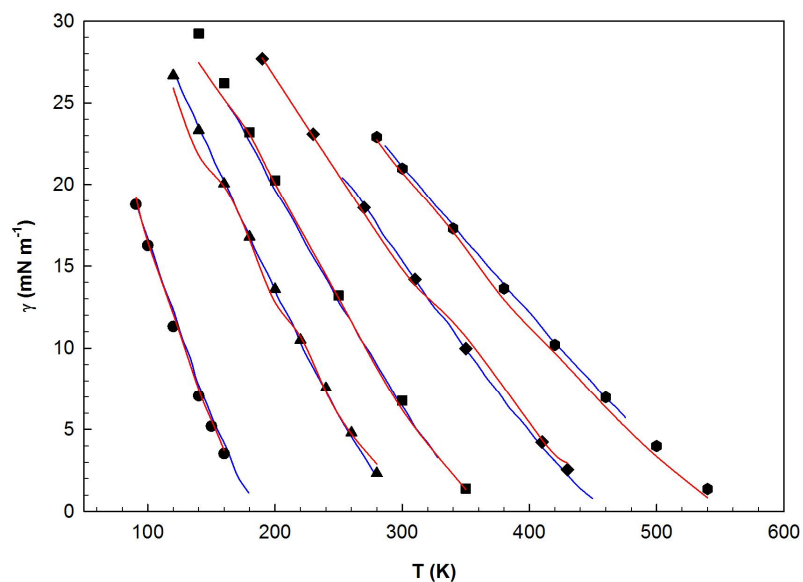
Fig. 4. The Calculated surface tension of n-alkanes C_1, C_2, C_3, C_5 and C_8 (left to right) in this work; the MPR-DFT (red line) and the results from Ref. [20] (blue line). The symbols are the experimental values.
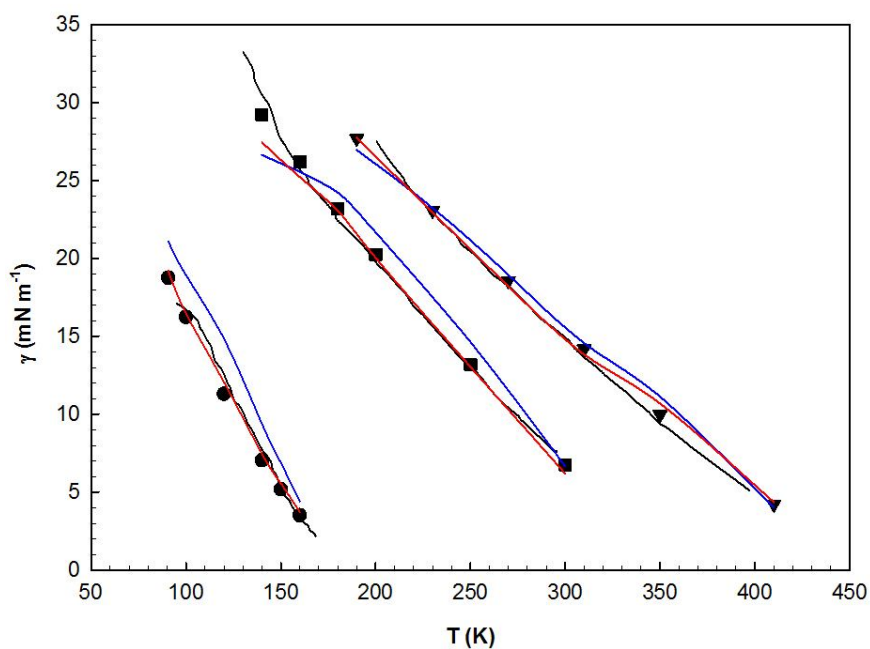
Fig. 5. The Calculated surface tension of n-alkanes C_1, C_3 and C_5 (left to right) in this work; the MPR-DFT (red line), the PR-DFT (blue line); and the data from Ref. [19] (black line). The symbols show the corresponding experimental values [35].

SAFT-BACK-DFT which is in a good agreement with the experiment in whole range of temperature.

CONCLUSIONS

DFT in conjunction with the MPR EoS was used to predict the surface tension of n-alkanes (C_1-C_{10}), and compared with the PR EoS. The accuracy of the calculated surface tension with DFT approach significantly depends on the EoS which is used to calculate the surface tension. It was shown that the MPR EoS provides a superior performance compared with the PR EoS in predicting the equilibrium values of the pressure and the liquid and vapor volumes. The density profile of n-alkanes which strongly depends on the intermolecular forces in the interfacial region of liquid-vapor phases was calculated for n-alkanes in the temperature range from triple point to near critical point. The results show that the interfacial layer thickness decreases with increase in the chain length of normal alkanes (C_1-C_{10}) and increases with temperature. This can be attributed to the weak intermolecular forces between the short chain n-alkanes with respect to the long chains.

It was shown that the MPR-DFT method can better predict the experimental surface tensions with regard to the PR-DFT. The maximum average absolute relative deviation in the calculation of the surface tension by MPR-DFT is 6% which is lower than the predicted values by PR-DFT. Comparison of the calculated surface tensions values using the MPR-DFT, the PR-DFT, the SAFT-BACK-DFT and the simulation indicates that the MPR –DFT method is a good candidate for predicting the surface tension of n-alkanes (C_1-C_{10}) in the limit of the experimental errors.

REFERENCES

[1] Stahl, E.; Quirin, K. -W., Gerard, D., Dense gases for extraction and refining: Springer Science & Business Media; 2012.

[2] Ceotto, D., Empirical equation for predicting the surface tension of some liquid metals at their melting point. *Russ. J. Phys. Chem. A.* **2014**, *88*, 1269-1272, DOI: 10.1134/S0036024414070073.

[3] Santos, M. S. C.; Reis, J. C. R., A semi-empirical equation for describing the surface tension of aqueous organic liquid mixtures. *Fluid Phase Equilib.* **2016**, *423*, 172-180, DOI: 10.1016/j.fluid.2016.04.025.

[4] Ceotto, D., Empirical relation between surface tension and density for some pure liquid metals. *Russ. J. Phys. Chem. A.* **2015**, *89*, 2327-2330, DOI: 10.1134/S0036024415130099.

[5] Ghatee, M. H.; Zare, M.; Zolghadr, A. R.; Moosavi, F., Temperature dependence of viscosity and relation with the surface tension of ionic liquids. *Fluid Phase Equilib.* **2010**, *291*, 188-194, DOI: 10.1016/j.fluid.2010.01.010.

[6] Keck, P. H.; Van Horn, W., The surface tension of liquid silicon and germanium. *Phys. Rev.* **1953**, *91*, 512-513, DOI: 10.1103/PhysRev.91.512.

[7] Allen, C. A.; Watts, K. C.; Ackman, R. G., Predicting the surface tension of biodiesel fuels from their fatty acid composition. *J. Am. Oil Chem. Soc.* 1999, *76*, 317-323, DOI: 10.1007/s11746-999-0238-5.

[8] Brock, J. R.; Bird, R. B., Surface tension and the principle of corresponding states. *AIChE J.* **1955**, *1*, 174-177, DOI: 10.1002/aic.690010208.

[9] Queimada, A.; Marrucho, I. M.; Coutinho, J., Surface tension of pure heavy n-alkanes: a corresponding states approach. *Fluid Phase Equilib.* **2001**, *183*, 229-238, DOI: 10.1016/S0378-3812(01)00434-4.

[10] Toxvaerd, S., Perturbation theory for nonuniform fluids: Surface tension. *J. Chem. Phys.* **1971**, *55*, 3116-3120, DOI: 10.1063/1.1676556.

[11] Haile, J.; Gray, C.; Gubbins, K., Theory of surface tension for molecular liquids. II. Perturbation theory calculations. *J. Chem. Phys.* **1976**, *64*, 2569-2578, DOI: 10.1063/1.432509.

[12] Zuo, Y. -X.; Stenby, E. H., A linear gradient theory model for calculating interfacial tensions of mixtures. *J. Colloid Interface Sci.* **1996**, *182*, 126-132, DOI: 10.1006/jcis.1996.0443.

[13] Lin, H.; Duan, Y.; Zhang, J., Simplified gradient theory modeling of the surface tension for binary mixtures. *Int. J. Thermophys.* **2008**, *29*, 423-433, DOI: 10.1007/s10765-007-0360-2.

[14] Ebner, C.; Saam, W.; Stroud, D., Density-functional theory of simple classical fluids. I. Surfaces. *Phys. Rev. A.* **1976**, *14*, 2264-2273, DOI: https://doi.org/10.1103/PhysRevA.14.2264.

[15] Teixeira, P.; da Gama, M. T., Density-functional theory for the interfacial properties of a dipolar fluid. *J. Phys.: Condens. Matter.* **1991**, *3*, 111, DOI: 10.1088/0953-8984/3/1/009.

[16] Forsman, J.; Woodward, C. E.; Trulsson, M., A classical density functional theory of ionic liquids. *J. Phys. Chem. B.* **2011**, *115*, 4606-4612.

[17] Gloor, G. J.; Blas, F. J.; del Río, E. M. N.; de Miguel, E.; Jackson, G., A SAFT-DFT approach for the vapour–liquid interface of associating fluids. *Fluid Phase Equilib.* **2002**, *194*, 521-530, DOI: 10.1016/S0378-3812(01)00774-9.

[18] Tang, X.; Gross, J., Density functional theory for calculating surface tensions with a simple renormalization formalism for the critical point. *J. Supercrit. Fluids.* **2010**, *55*, 735-742, DOI: 10.1016/j.supflu.2010.09.041.

[19] Maghari, A., Najafi, M., On the Calculation of Surface Tensions of n-Alkanes Using the Modified SAFT-BACK-DFT Approach. J. Solution Chem. 2010, 39(1), 31-41, DOI: 10.1007/s10953-009-9480-6.

[20] Li, Z.; Firoozabadi, A., Interfacial tension of nonassociating pure substances and binary mixtures by density functional theory combined with Peng-Robinson equation of state. *J. Chem. Phys.* **2009**, *130*, 154108, DOI: 10.1063/1.3100237.

[21] von Müller, A.; Leonhard, K., Surface tension calculations by means of a PCP-SAFT-DFT formalism using equation of state parameters from quantum mechanics. *Fluid Phase Equilib.* **2013**, *356*, 96-101, DOI: 10.1016/j.fluid.2013.07.005.

[22] Gloor, G. J.; Jackson, G.; Blas, F. J.; del Rıo, E. M.; de Miguel, E., An accurate density functional theory for the vapor-liquid interface of associating chain molecules based on the statistical associating fluid theory for potentials of variable range. *J. Chem. Phys.* **2004**, *121*, 12740-12759, DOI: 10.1063/1.1807833.

[23] Gloor, G. J.; Jackson, G.; Blas, F.; Del Rio, E. M.; De Miguel, E., Prediction of the vapor-liquid interfacial tension of nonassociating and associating fluids with the SAFT-VR density functional theory. *J. Phy. Chem. C.* **2007**, *111*, 15513-15522, DOI: 10.1021/jp072344i.

[24] Kahl, H.; Winkelmann, J., Modified PT-LJ-SAFT Density Functional Theory: I. Prediction of surface properties and phase equilibria of non-associating fluids. *Fluid Phase Equilib.* **2008**, *270*, 50-61, DOI: 10.1016/j.fluid.2008.06.002.

[25] Gross, J., A density functional theory for vapor-liquid interfaces using the PCP-SAFT equation of state. *J. Chem. Phys.* **2009**, *131*, 204705-204717, DOI: 10.1063/1.3263124.

[26] Llovell, F.; Galindo, A.; Blas, F. J.; Jackson, G., Classical density functional theory for the prediction of the surface tension and interfacial properties of fluids mixtures of chain molecules based on the statistical associating fluid theory for potentials of variable range. *J. Chem. Phys.* **2010**, *133*, 024704-024723, DOI: 10.1063/1.3449143.

[27] Llovell, F.; Mac Dowell, N.; Blas, F. J.; Galindo, A.; Jackson, G., Application of the SAFT-VR density functional theory to the prediction of the interfacial properties of mixtures of relevance to reservoir engineering. *Fluid Phase Equilib.* **2012**, *336*, 137-150, DOI: 10.1016/j.fluid.2012.07.033.

[28] Feyzi, F.; Riazi, M.; Shaban, H.; Ghotbi, S., Improving cubic equations of state for heavy reservoir fluids and critical region. *Chem. Eng. Commun.* **1998**, *167*, 147-166, DOI: 10.1080/00986449808912698.

[29] Peng, D. -Y.; Robinson, D. B., A new two-constant equation of state. *Ind. Eng. Chem. Fundam.* **1976**, *15*, 59-64, DOI: 10.1021/i160057a011.

[30] Vargaftik, N. B.; Vinogradov, Y. K.; Yargin, V. S., Handbook of physical properties of liquids and gases: Pure Substances and Mixtures: Springer-Verlag Berlin Heidelberg; 1975.

[31] Perry, R. H.; Green, D. W., Perry's chemical engineers' handbook: McGraw-Hill Professional; 1999.

[32] Vargaftik, N. B.; Vinogradov, Y. K.; Yargin, V. S., Handbook of physical properties of liquids and gases: Pure Substances and Mixtures, Springer-Verlag Berlin Heidelberg; 1975.

[33] Hohenberg, P.; Kohn, W., Inhomogeneous electron gas. *Phys. Rev.* **1964**, *13*, B864-B871, DOI: 10.1103/PhysRev.136.B864.

[34] Mermin, N. D., Thermal properties of the

inhomogeneous electron gas. *Phys. Rev.* **1965**, *137*, A1441-A1443, DOI: 10.1103/PhysRev.137.A1441.

[35] Rowlinson, J.; Widom, B., Molecular Theory of Capillarity, The International Series of Monographs on Chemistry: Clarendon Press, Oxford, 1982.

[36] Wu, J., Density functional theory for chemical engineering: From capillarity to soft materials. *AIChE J.* **2006**, *52*, 1169-1193, DOI: 10.1002/aic.10713.

[37] Fu, D.; Lu, J. -F.; Liu, J. -C., Li, Y. -G., Prediction of surface tension for pure non-polar fluids based on density functional theory. *Chem. Eng. Sci.* **2001**, *56*, 6989-6996, DOI: 10.1016/S0009-2509(01)00331-1.

[38] Lu, J. -F.; Fu, D.; Liu, J. -C.; Li, Y. -G., Application of density functional theory for predicting the surface tension of pure polar and associating fluids. *Fluid Phase Equilib.* **2002**, *194*, 755-769, DOI: 10.1016/S0378-3812(01)00692-6.

[39] Lias, S.; Bartmess, J.; Liebman, J.; Holmes, J.; Levin, R.; Mallard, W., NIST Chemistry WebBook, NIST Standard Reference Database Number 69. National Institute of Standards and Technology, Gaithersburg MD2003.

[40] Amat, M. A.; Rutledge, G. C., Liquid-vapor equilibria and interfacial properties of n-alkanes and perfluoroalkanes by molecular simulation. *J. Chem. Phys.* **2010**, *132*, 114704, DOI: 10.1063/1.3356219.

[41] Nath, S. K.; Escobedo, F. A.; de Pablo, J. J., On the simulation of vapor-liquid equilibria for alkanes. *J. Chem. Phys.* **1998**, *108*, 9905-9911, DOI: 10.1063/1.476429.

[42] Mendoza, F. N.; Lopez-Rendon, R.; Lopez-Lemus, J.; Cruz, J.; Alejandre, J., Surface tension of hydrocarbon chains at the liquid-vapour interface. *Mol. Phys.* **2008**, *106*, 1055-1059, DOI: 10.1080/00268970802119694.